Intrinsic decoherence dynamics in smooth Hamiltonian systems: Quantum-classical correspondence

Jiangbin Gong and Paul Brumer
Chemical Physics Theory Group, Department of Chemistry, University of Toronto, Toronto, Canada M5S 3H6
(Received 7 March 2003; published 1 August 2003)

A direct classical analog of the quantum dynamics of intrinsic decoherence in Hamiltonian systems, characterized by the time dependence of the linear entropy of the reduced density operator, is introduced. The similarities and differences between the classical and quantum decoherence dynamics of an initial quantum state are exposed using both analytical and computational results. In particular, the classicality of early-time intrinsic decoherence dynamics is explored analytically using a second-order perturbative treatment, and an interesting connection between decoherence rates and the stability nature of classical trajectories is revealed in a simple approximate classical theory of intrinsic decoherence dynamics. The results offer deeper insights into decoherence, dynamics of quantum entanglement, and quantum chaos.

DOI: 10.1103/PhysRevA.68.022101 PACS number(s): 03.65.Yz, 03.65.Ud, 05.45.Mt

I. INTRODUCTION

Quantum dynamics induces unitary transformations in a Hilbert space, but most often it is only the dynamics projected onto a Hilbert *subspace* that is of interest. In general, this reduced dynamics is nonunitary and therefore displays decoherence [1]. For example, if a system of interest is coupled to a bath, then averaging over the bath degrees of freedom introduces decoherence in the system dynamics. Likewise, in an isolated system, the reduced dynamics of a subsystem of this isolated system can display decoherence. We have termed decoherence in the latter case "*intrinsic decoherence*" since it does not involve an external bath [2].

Understanding decoherence is of crucial importance to a variety of modern fields such as quantum information processing [3] and quantum control of atomic and molecular processes [4–6]. Our interest here is in the quantum-classical correspondence (QCC) between classical and quantum descriptions of the *dynamics* of decoherence. Specifically, we consider an initial quantum state subjected to either quantum or classical dynamics and compare the time evolution of the decoherence in both cases. We note that the formal theory of correspondence between quantum dynamics and classical Liouville dynamics [7] suggests that classical Liouville dynamics projected onto a subspace should also display decoherence. That is, as in the quantum case, the classical Liouville dynamics considered in the entire phase space is unitary and the classical Liouville dynamics projected onto a subspace is nonunitary. We, therefore, expect that the reduced classical Liouville dynamics propagated classically will show decoherence dynamics that is, at least qualitatively, parallel to that seen in the reduced quantum dynamics insofar as the loss of phase information, entropy production, etc. In the case of bath-induced decoherence, we recently showed analytically that (a) one can indeed introduce a direct classical analog of quantum decoherence, and (b) examining the dynamics of decoherence classically gives deeper insights into both the dynamics of decoherence described quantum mechanically and into the conditions for the QCC in decoherence dynamics [8].

Here we extend these considerations to intrinsic decoherence, both analytically and computationally. Specifically, in this paper we study the QCC in the dynamics of intrinsic decoherence in smooth Hamiltonian systems, with an emphasis on the usefulness of classical dynamics in describing intrinsic decoherence. In particular, the classicality of early-time intrinsic decoherence dynamics is studied using a second-order perturbative treatment, and the interesting connection between decoherence rates at later times and the stability properties of classical trajectories is revealed by considering a simple approximate classical theory of intrinsic decoherence dynamics. The analytic and computational results shed more light on decoherence, dynamics of quantum entanglement, and quantum chaos. This study is also of interest to semiclassical decoherence studies [9], e.g., semiclassical descriptions of intrinsic decoherence dynamics in large molecular systems [2].

This paper is organized as follows. In Sec. II, we introduce a second-order perturbation theory in an effort to understand the QCC in early-time intrinsic decoherence dynamics. For simplicity we focus upon two degree-of-freedom systems, but the extension to larger systems is straightforward. Computational results of two sample cases in coupled-oscillator model systems, which strongly support the physical picture afforded by the perturbative treatment, are presented in Sec. III. Then, a classical theory of intrinsic decoherence dynamics for initially localized states is derived in Sec. IV. In the same section, detailed computational studies using this simple theory are carried out for the quartic oscillator model and one of its variants. Discussions and a summary comprise Sec. V.

II. EARLY-TIME INTRINSIC DECOHERENCE DYNAMICS

Consider a conservative system composed of two subsystems, with the total Hamiltonian given by

$$H(Q,P,q,p)=\frac{P^2}{2}+\frac{p^2}{2}+V_1(Q)+V_2(q)+V_{12}(Q,q), \tag{1}$$

where (Q,P) and (q,p) are dimensionless phase-space conjugate variables, V_i is the potential of the ith subsystem, and $V_{12}(Q,q)$ describes arbitrary coupling between the two sub-

systems. As the system evolves, the total system wave function $|\psi(t)\rangle$ becomes inseparable due to quantum entanglement, even if it is initially separable in Q and q. As a result, measuring a subsystem would collapse the system wave function and therefore affect the properties of the other subsystem. Similarly, ignoring a subsystem decoheres the other one. The degree of intrinsic decoherence, which is induced by, and is a manifestation of, quantum entanglement between the two subsystems, can be measured by a well-known quantity: the quantum linear entropy [10]

$$S_{\mathrm{q}}=1-\mathrm{Tr}_1(\hat{\tilde{\rho}}^2), \tag{2}$$

where Tr_i denotes a trace over the ith subsystem, and $\hat{\tilde{\rho}} \equiv \mathrm{Tr}_2[|\psi(t)\rangle\langle\psi(t)|]$ is the reduced density operator for the first subsystem. An increase in S_{q} suggests an increase of $1/(1-S_{\mathrm{q}})$, which gives the number of orthogonal quantum states that are incoherently populated if the second subsystem is ignored. Below we choose q,p as the "bath" variables and P,Q as the system variables.

Let $\rho_c(Q,P,q,p,t)$ denote the phase-space distribution function evolved classically, and $\rho_W(Q,P,q,p,t)$ denote the quantum (Wigner) phase-space distribution function. Their time evolution equations are given by

$$\frac{\partial \rho_c}{\partial t}=\{H,\rho_c\}, \tag{3}$$

$$\frac{\partial \rho_W}{\partial t}=\{H,\rho_W\}_M, \tag{4}$$

where $\{\cdot\}$ denotes the classical Poisson bracket and $\{\cdot\}_M$ denotes the quantum Moyal bracket [11]. We define classical and quantum reduced distribution functions as

$$\tilde{\rho}_c(Q,P,t)\equiv\int \rho_c(Q,P,q,p,t)dq\,dp, \tag{5}$$

$$\tilde{\rho}_W(Q,P,t)\equiv\int \rho_W(Q,P,q,p,t)dq\,dp. \tag{6}$$

Since

$$S_{\mathrm{q}}(t)=1-2\pi\hbar\int \tilde{\rho}_W^2(Q,P,t)dQ\,dP, \tag{7}$$

where $\hbar$ is the effective Planck constant, we can define a classical analog [denoted $S_c(t)$] to $S_{\mathrm{q}}(t)$ by replacing $\tilde{\rho}_W$ with $\tilde{\rho}_c$. That is,

$$S_c(t)\equiv 1-2\pi\hbar\int \tilde{\rho}_c^2(Q,P,t)dQ\,dP. \tag{8}$$

The main focus here is to compare $S_c(t)$ with $S_{\mathrm{q}}(t)$, i.e., the classical vs quantum evolution of the intrinsic decoherence dynamics, as measured by the classical vs quantum entropy.

Perturbative treatments have proved to be very useful in understanding decoherence dynamics [8,12–14]. Here, to analytically examine classical vs quantum intrinsic decoherence dynamics at early times, we apply the perturbative approach developed in our previous work [8] to the case of intrinsic decoherence dynamics. Specifically, consider a second-order perturbative expansion with respect to the time variable t for both S_{q} and S_c, i.e.,

$$S_c(t)=S_c(0)+\frac{t}{\tau_{c,1}}+\frac{t^2}{\tau_{c,2}^2}+\cdots,$$

$$S_{\mathrm{q}}(t)=S_{\mathrm{q}}(0)+\frac{t}{\tau_{\mathrm{q},1}}+\frac{t^2}{\tau_{\mathrm{q},2}^2}+\cdots. \tag{9}$$

Then, from the classical and quantum dynamics of the entire system one obtains

$$\frac{1}{\tau_{c,1}}=-4\pi\hbar\int \tilde{\rho}_c(Q,P,0)\int\{H,\rho_c(Q,P,q,p,0)\}\times dq\,dp\,dQ\,dP, \tag{10}$$

$$\frac{1}{\tau_{\mathrm{q},1}}=-4\pi\hbar\int \tilde{\rho}_W(Q,P,0)\int\{H,\rho_W(Q,P,q,p,0)\}_M\times dq\,dp\,dQ\,dP, \tag{11}$$

$$\frac{1}{\tau_{c,2}^2}=-2\pi\hbar\int \tilde{\rho}_c(Q,P,0)\int\{H,\{H,\rho_c(Q,P,q,p,0)\}\}\times dq\,dp\,dQ\,dP -2\pi\hbar\int\left[\int\{H,\rho_c(Q,P,q,p,0)\}dq\,dp\right]^2 dQ\,dP, \tag{12}$$

and

$$\frac{1}{\tau_{\mathrm{q},2}^2}=-2\pi\hbar\int \tilde{\rho}_W(Q,P,0)\int\{H,\{H,\rho_W(Q,P,q,p,0)\}_M\}_M\times dq\,dp\,dQ\,dP -2\pi\hbar\int\left[\int\{H,\rho_W(Q,P,q,p,0)\}_M dq\,dp\right]^2 dQ\,dP. \tag{13}$$

Further, using the definitions of the classical Poisson and quantum Moyal brackets and assuming that initial classical and quantum distribution functions are identical and separable, i.e.,

$$\rho_c(Q,P,q,p,0)=\rho_W(Q,P,q,p,0)=\tilde{\rho}_1^0(Q,P)\tilde{\rho}_2^0(q,p), \tag{14}$$

we have

$$\frac{1}{\tau_{c,1}}=\frac{1}{\tau_{\mathrm{q},1}}=0, \tag{15}$$

$$\frac{1}{\tau_{c,2}^2}=2\pi\hbar\int\left[\frac{\partial\tilde{\rho}_1^0(Q,P)}{\partial P}\right]^2 C(0,0)dQ\,dP, \tag{16}$$

and

$$\frac{1}{\tau_{q,2}^2}=\frac{1}{\tau_{c,2}^2}+2\pi\hbar\int\sum_{l_1\neq l_2\geqslant 0}\frac{[\hbar/(2i)]^{(2l_1+2l_2)}}{(2l_1+1)!(2l_2+1)!}\times\frac{\partial^{(2l_1+1)}\tilde{\rho}_1^0(Q,P)}{\partial P^{(2l_1+1)}}\frac{\partial^{(2l_2+1)}\tilde{\rho}_1^0(Q,P)}{\partial P^{(2l_2+1)}}C(l_1,l_2)dQ\,dP, \tag{17}$$

where $C(l_1,l_2)$ is a correlation function given by

$$C(l_1,l_2)\equiv\left\langle\frac{\partial^{(2l_1+1)}V(Q,q)}{\partial Q^{(2l_1+1)}}\frac{\partial^{(2l_2+1)}V(Q,q)}{\partial Q^{(2l_2+1)}}\right\rangle_{\tilde{\rho}_2^0}-\left\langle\frac{\partial^{(2l_1+1)}V(Q,q)}{\partial Q^{(2l_1+1)}}\right\rangle_{\tilde{\rho}_2^0}\left\langle\frac{\partial^{(2l_2+1)}V(Q,q)}{\partial Q^{(2l_2+1)}}\right\rangle_{\tilde{\rho}_2^0}. \tag{18}$$

Here $\langle\cdot\rangle_{\tilde{\rho}_2^0}$ denotes the ensemble average over the zero-time "bath distribution function" $\tilde{\rho}_2^0(q,p)$. It is worth emphasizing that in our derivations we have used the same initial state for the classical and quantum dynamics.

Equation (15) shows that the zero first-order linear entropy increase rate, i.e., $1/\tau_{q,1}=0$, has a strict classical analog. Further, Eq. (16) indicates that classical Liouville dynamics also predicts a second-order entropy production rate $1/\tau_{c,2}^2$ that is the analog of the second-order quantum decoherence rate $1/\tau_{q,2}^2$. Thus, we can identify two categories of early-time intrinsic decoherence dynamics: *classical* if $\tau_{c,2}\approx\tau_{q,2}$, and *nonclassical* if $\tau_{q,2}$ appreciably differs from $\tau_{c,2}$.

To simplify Eqs. (16) and (17), we introduce the Fourier transform [denoted $F(Q_1,Q_2)$] of $\tilde{\rho}_1^0(Q,P)$, i.e.,

$$F(Q_1,Q_2)\equiv\int\tilde{\rho}_1^0(\overline{Q},P)\exp\left[\frac{i\Delta QP}{\hbar}\right]dP, \tag{19}$$

where $\overline{Q}\equiv(Q_1+Q_2)/2$ and $\Delta Q=Q_1-Q_2$. We then obtain

$$\frac{1}{\tau_{c,2}^2}=\frac{1}{\hbar^2}\int|F(Q_1,Q_2)|^2\Delta Q^2C(0,0)dQ_1\,dQ_2, \tag{20}$$

and

$$\frac{1}{\tau_{q,2}^2}=\frac{1}{\tau_{c,2}^2}+\frac{1}{\hbar^2}\int|F(Q_1,Q_2)|^2\sum_{l_1\neq l_2\geqslant 0}\frac{\Delta Q^{(2l_1+2l_2+2)}}{(2l_1+1)!(2l_2+1)!}\times\frac{1}{2^{(2l_1+2l_2)}}C(l_1,l_2)dQ_1\,dQ_2. \tag{21}$$

Equations (20) and (21) are general results. For the special case of $V_{12}(Q,q)=f(Q)g(q)$, Eqs. (20) and (21) can be rewritten in a simple and more enlightening form:

$$\frac{1}{\tau_{c,2}^2}=\frac{\langle g^2(q)\rangle_{\tilde{\rho}_2^0}-\langle g(q)\rangle_{\tilde{\rho}_2^0}^2}{\hbar^2}\times\int|F(Q_1,Q_2)|^2\Delta Q^2\left[\frac{df(\overline{Q})}{dQ}\right]^2dQ_1\,dQ_2, \tag{22}$$

and

$$\frac{1}{\tau_{q,2}^2}=\frac{\langle g^2(q)\rangle_{\tilde{\rho}_2^0}-\langle g(q)\rangle_{\tilde{\rho}_2^0}^2}{\hbar^2}\times\int|F(Q_1,Q_2)|^2\Delta Q^2\left[\frac{\Delta f(\overline{Q})}{\Delta Q}\right]^2dQ_1\,dQ_2, \tag{23}$$

where $\Delta f(\overline{Q})/\Delta Q$ is the finite-difference function,

$$\frac{\Delta f(\overline{Q})}{\Delta Q}\equiv\frac{f(\overline{Q}+\Delta Q/2)-f(\overline{Q}-\Delta Q/2)}{\Delta Q}=\frac{f(Q_1)-f(Q_2)}{Q_1-Q_2}. \tag{24}$$

As a result we have the following.

(1) If $f(Q)$ depends only linearly or quadratically upon the coupling coordinate Q, a common approximation, then $(1/\tau_{q,2}^2-1/\tau_{c,2}^2)=0$ for any initial state. That is, in this case there exists perfect QCC in early-time dynamics of intrinsic decoherence, regardless of $\hbar$, and irrespective of the potentials $V_1(Q)$ and $V_2(q)$.

(2) Even in the case of highly nonlinear $f(Q)$, as long as $F(Q_1,Q_2)$ decays fast enough with $|Q_1-Q_2|$ such that $\Delta f/\Delta Q\approx df/dQ$, the QCC would still be excellent. The smaller the $\hbar$, the more rigorous is this requirement.

(3) If $\Delta f/\Delta Q$ differs significantly from df/dQ over the Q-coordinate scale of the initial state, quantum entropy production can be totally unrelated to classical entropy production. Such cases of poor QCC are of fundamental interest, but are not the focus of this paper.

The second-order perturbative treatment is most reliable for early-time dynamics and for relatively weak decoherence. The above results are particularly significant for studies on the control of intrinsic decoherence, where early-time dynamics of weak decoherence is important. In these circumstances it is useful to understand the extent to which (quantum) intrinsic decoherence is equivalent to classical entropy production, i.e., to increasing $S_c(t)$. In particular, if there exists good correspondence between classical and quantum decoherence dynamics, then the essence of decoherence control is equivalent to the suppression of classical entropy production, and various classical tools may be considered to achieve decoherence control. If not, then fully quantum tools are required.

The above perturbation results clearly demonstrate that quantum dynamics of intrinsic decoherence has a direct ana-

log in classical Liouville dynamics. This rather intriguing result motivates us to computationally examine the QCC in the dynamics of intrinsic decoherence over all time scales.

III. COMPUTATIONAL RESULTS: TWO SAMPLE CASES

To computationally examine the QCC in the dynamics of intrinsic decoherence, we consider coupled-oscillator model systems with smooth Hamiltonians. In all the model systems studied below, we choose

$$V_1(Q)+V_2(q)=\frac{\beta}{4}(Q^4+q^4), \tag{25}$$

where $\beta=0.01$. Since $V_1(Q)$ and $V_2(q)$ have no simple harmonic terms, any observed agreement between classical and quantum behaviors cannot be attributed to the similarity between classical and quantum harmonic-oscillator dynamics. If the coupling potential $V_{12}(Q,q)$ is quadratic in both Q and q, i.e., $V_{12}(Q,q)=\alpha Q^2q^2/2$, then the resultant coupled-oscillator system is the well known quartic oscillator model [15–17]. Because this model is well-studied and can display strongly chaotic (e.g., $\alpha=1.0$, $\beta=0.01$) or integrable (e.g., $\alpha=0.03$, $\beta=0.01$) dynamics, it is used in Sec. IV as an ideal model to study the QCC in intrinsic decoherence dynamics for both integrable and chaotic cases.

Our perturbation-theory approach predicts good classical-quantum agreement at short times for some potentials and initial conditions and poor agreement for others. We examine both these cases computationally.

It suffices to consider one case of poor agreement, since poor QCC at early times invariably translates to similar behavior at later times. Consider then $V_{12}(Q,q)$ to be some highly nonlinear potential. Computations of the quantum dynamics and thus the time dependence of $S_{\mathrm{q}}(t)$ are straightforward [16]. $S_c(t)$ is computed directly using the Monte Carlo simulations with an importance sampling technique [where the Monte Carlo simulations are based upon Eq. (27) below]. From the analytical results above we see that $V_{12}(Q,q)$ and the scale of the initial state play decisive roles in the QCC in early-time intrinsic decoherence dynamics. In particular, we expect poor QCC if $V_{12}(Q,q)=f(Q)g(q)$ differs significantly from a linear or quadratic function of Q such that $\Delta f/\Delta Q$ differs significantly from (df/dQ) over the Q-coordinate scale (i.e., the support) of the initial state. To confirm this computationally we consider $f(Q)g(q)=\sin^2(10Q)q^2$, with the initial distribution functions of the two subsystems given by

$$\tilde{\rho}_1^0(Q,P)=\frac{1}{\pi\hbar}\exp\left[-\frac{(Q-Q_0)^2}{2\sigma_Q^2}-\frac{(P-P_0)^2}{2\sigma_P^2}\right],$$

$$\tilde{\rho}_2^0(q,p)=\frac{1}{\pi\hbar}\exp\left[-\frac{(q-q_0)^2}{2\sigma_q^2}-\frac{(p-p_0)^2}{2\sigma_p^2}\right]. \tag{26}$$

Here the dimensionless effective Planck constant is chosen to be $\hbar=0.005$ throughout, except for one case in Sec. V, and $\sigma_Q/25=25\sigma_P=\sqrt{\hbar/2}$, $\sigma_q=\sigma_p=\sqrt{\hbar/2}$, $Q_0=0.5$, $P_0=0.5$, $q_0=0$, with $H(Q_0,P_0,q_0,p_0)=0.24$. Note that $\tilde{\rho}_1^0(Q,P)$ is strongly squeezed in P and that this initial distribution function is considerably delocalized in Q. Further, since $|f(Q)|=|\sin^2(10Q)|\leqslant 1.0$, $|\Delta Q||df/dQ|$ can be much larger than $|\Delta f(Q)|$. Thus, for this case the perturbation result predicts that at early times there can be substantial classical entropy production with insignificant quantum decoherence. As shown in Fig. 1, this is nicely confirmed by the numerical results of $S_{\mathrm{q}}(t)$ and $S_c(t)$. In particular, Fig. 1 shows that at $t=1.0$, $S_c(t)$ (discrete points) is ~ 0.9 while $S_{\mathrm{q}}(t)$ (solid line) is still less than 0.2. Evidently, the QCC in this case is indeed very poor from the very beginning.

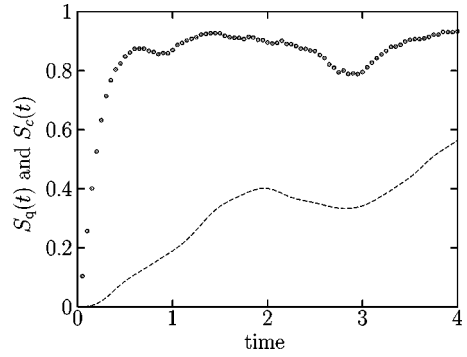

FIG. 1. A comparison between $S_{\mathrm{q}}(t)$ (dashed line) and $S_c(t)$ (discrete circular points) in the first sample case. The coupling potential is highly nonlinear such that at early times classical entropy production is much faster than quantum entropy production. See the text for details. All variables are in dimensionless units.

There remains then the important question of the quantitative degree of the QCC in circumstances where our perturbative analysis predicts good short-time QCC. In particular, it is important to investigate whether or not good QCC predicted perturbatively remains for a considerable amount of time. If so, then the perturbative treatment provides a useful guide to our understanding of the QCC in intrinsic decoherence dynamics. If not, then our perturbative results make sense only for extremely weak decoherence. Dramatically, our computational studies strongly support our analytical perturbation results, even in the presence of significant decoherence. For example, consider the case, where the parameters for the initial state are the same as in the previous case (therefore the initial state is also much delocalized), but the coupling potential is given by $V_{12}(Q,q)=Q^2\sin^2(q)$. This coupling potential is highly nonlinear in q but still quadratic in Q. In accord with the second-order perturbation results, such a coupling potential should still give rise to good early-time QCC in the intrinsic decoherence dynamics of the first subsystem. This is confirmed by the quantitative comparison between $S_{\mathrm{q}}(t)$ and $S_c(t)$ shown in Fig. 2. More importantly, Fig. 2 shows that outstanding QCC remains even when both $S_{\mathrm{q}}(t)$ and $S_c(t)$ have increased to close to their saturation value of unity. Numerous other computational results (not shown) are consistent with the two cases shown here.

These results show the usefulness of the second-order perturbation theory in understanding the QCC in intrinsic decoherence dynamics emanating from squeezed initial states. Also of interest is intrinsic decoherence dynamics associated

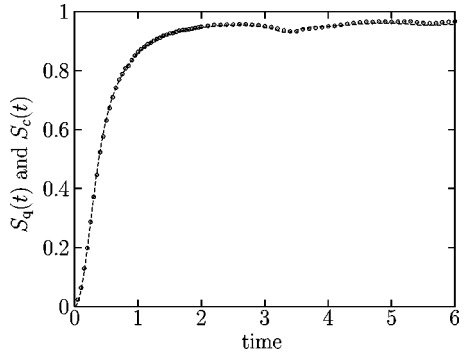

FIG. 2. A comparison between $S_q(t)$ (dashed line) and $S_c(t)$ (discrete circular points) in the second sample case. The coupling potential is highly nonlinear in terms of the position of the second subsystem, but is quadratic in terms of the position of the first subsystem, resulting in excellent quantum-classical correspondence in intrinsic decoherence dynamics even though the initial distribution function of the first subsystem is considerably delocalized. See the text for details. All variables are in dimensionless units.

with sufficiently localized initial states, which, in accord with the previous perturbation results, should display excellent early-time QCC for any coupling potential $V_{12}(Q,q)$. We now computationally examine the QCC at later times for localized states as initial conditions and explain the results in terms of a simple classical theory of intrinsic decoherence dynamics.

IV. LOCALIZED INITIAL STATES

A. Simple classical approach

Below we show that $S_q(t)$ and $S_c(t)$ are often in excellent agreement, over large time scales, for initially localized states, significantly extending the perturbation-theory result. In doing so, we compare the quantum $S_q(t)$ with full classical mechanics as well as with a simple classical theory derived in this section. The latter provides further insight into the origins of increasing $S_c(t)$.

To derive the simplified classical result, we first use Liouville's theorem to reexpress $S_c(t)$ as

$$\begin{aligned} S_c(t) &= 1-2\pi\hbar \int\int \rho_c(Q(t),P(t),q(t),p(t),t) \\ &\quad \times \rho_c(Q(t),P(t),q',p',t)dq'\,dp'\,dQ(t)dP(t) \\ &\quad \times dq(t)dp(t) \\ &= 1-2\pi\hbar \int\int \rho_c(Q,P,q,p,0)\rho_c(Q(t),P(t),q',p',t) \\ &\quad \times dq'\,dp'dQ\,dPdq\,dp \\ &= 1-2\pi\hbar \int\int \rho_c(Q,P,q,p,0)\rho_c(Q'',P'',q'',p'',0) \\ &\quad \times dq'\,dp'dQ\,dPdq\,dp, \end{aligned} \tag{27}$$

where $(Q(t),P(t),q(t),p(t))$ is the phase-space location of the trajectory emanating from (Q,P,q,p) at $t=0$, and (Q'',P'',q'',p'') is the phase-space location of the trajectory at time zero if the classical trajectory is propagated backwards from $(Q(t),P(t),q',p')$. Because the initial state $\rho_c(Q,P,q,p,0)$ is assumed highly localized in phase space, (Q'',P'',q'',p'') must be very close to (Q,P,q,p) in order for the term $\rho_c(Q,P,q,p,0)\rho_c(Q'',P'',q'',p'',0)$ in Eq. (27) to be appreciable and thus to contribute to $S_c(t)$. Hence a convenient approximation can be made: we assume that, at time t, only those backward trajectories near $(Q(t),P(t),q(t),p(t))$ need be taken into account. This means that we treat $Q''-Q$, $P''-P$, $q''-q$, $p''-p$, $\delta q' \equiv [q'-q(t)]$, and $\delta p' \equiv [p'-p(t)]$ as sufficiently small such that

$$\begin{aligned} Q'' &\approx Q + M_{13}(t)\,\delta q' + M_{14}(t)\,\delta p', \\ P'' &\approx P + M_{23}(t)\,\delta q' + M_{24}(t)\,\delta p', \\ q'' &\approx q + M_{33}(t)\,\delta q' + M_{34}(t)\,\delta p', \\ p'' &\approx p + M_{43}(t)\,\delta q' + M_{44}(t)\,\delta p', \end{aligned} \tag{28}$$

where M_{ij} $(i,j=1,2,3,4)$ is the stability matrix associated with the backward trajectories emanating from $(Q(t),P(t),q(t),p(t))$:

$$M_{ij} = \frac{\partial(Q,P,q,p)}{\partial(Q(t),P(t),q(t),p(t))}. \tag{29}$$

Although this approximation should be less reliable for chaotic systems, we demonstrate below that, it is, nonetheless, computationally useful in both integrable and chaotic cases.

For simplicity, we consider below a specific example in which $\tilde{\rho}_1^0(Q,P)$ and $\tilde{\rho}_2^0(q,p)$ are symmetric Gaussian states given by Eq. (26) with $\sigma_Q=\sigma_P=\sigma_q=\sigma_p\equiv\sigma=\sqrt{\hbar/2}$. Other distributions can be considered in an analogous fashion. Substituting Eqs. (26) and (28) into Eq. (27) and evaluating the integrals, we obtain

$$S_c(t) = 1-\frac{1}{2}\left\langle \frac{\exp\left[\dfrac{U^2X^2+V^2Y^2-2UVZ}{2\sigma^2(X^2Y^2-Z^2)}\right]}{\sqrt{X^2Y^2-Z^2}} \right\rangle_{\rho_c'}, \tag{30}$$

where

$$\begin{aligned} X &= M_{13}^2+M_{23}^2+M_{33}^2+M_{43}^2, \\ Y &= M_{14}^2+M_{24}^2+M_{34}^2+M_{44}^2, \\ Z &= M_{13}M_{14}+M_{23}M_{24}+M_{33}M_{34}+M_{43}M_{44}, \\ U &= (Q-Q_0)M_{14}+(P-P_0)M_{24}+(q-q_0)M_{34} \\ &\quad +(p-p_0)M_{44}, \\ V &= (Q-Q_0)M_{13}+(P-P_0)M_{23}+(q-q_0)M_{33} \\ &\quad +(p-p_0)M_{43}, \end{aligned} \tag{31}$$

and

$$\rho_c'(Q,P,q,p)=4\pi^2\hbar^2[\tilde{\rho}_1^0(Q,P)]^2[\tilde{\rho}_2^0(q,p)]^2. \quad (32)$$

Equations (30) and (31) indicate that the classical dynamics of intrinsic decoherence is closely related to the classical stability matrix elements averaged over a rescaled initial distribution function. This interesting connection provides insight into a variety of interesting aspects of quantum intrinsic decoherence dynamics [18–22]. For example, for chaotic dynamics in which classical trajectories are highly unstable and therefore in which $|M_{ij}|$ increases rapidly, $S_c(t)$ should increase much faster than for the case of integrable dynamics. This observation can, with the assumption that there is fairly good QCC in intrinsic decoherence dynamics, directly explain previous results on quantum signatures of classical chaos in the dynamics of quantum entanglement [18]. Further, because Eqs. (30) and (31) are expressed in terms of classical stability matrices, characteristics of the time dependence of $S_c(t)$ and therefore of $S_{\rm q}(t)$ can be easily related to the time and space fluctuations in the instability of classical trajectories.

B. Computational results: Localized initial states

Consider then the QCC over large time scales for localized initial states for both integrable and chaotic cases. To do so, we examine the quartic oscillator model as well as results where the coupling potential is replaced by the nonlinear potential $V_{12}(Q,q)=0.5Q^2q^2+Q^4q^2$. The initial states are chosen to be localized initial states, and both the full classical dynamics and the approximate time dependence of $S_c(t)$ in Eq. (30) are compared to the quantum result. Specifically, we realize the ensemble average in Eq. (30) by the Monte Carlo simulations, using only 2×10^4 sampling classical trajectories from which the stability matrix elements M_{ij} are evaluated. The initial Gaussian states are chosen symmetric with $\sigma=\sqrt{\hbar/2}=0.05$ and are sufficiently localized so that Eq. (28) should be a valid approximation. Full classical results for $S_c(t)$ (represented again by discrete circular points), which are much more demanding computationally, are also provided below.

Figures 3 and 4 compare results for $S_c(t)$ obtained from Eq. (30) and from exact classical results with $S_{\rm q}(t)$ (dashed line) for integrable and chaotic dynamics in the quartic oscillator model, respectively. A number of observations are in order. First, it is clear that in both cases the approximate $S_c(t)$ are in excellent agreement with the full classical results, confirming the utility of the simple model [Eq. (30)]. Second, both $S_c(t)$ and $S_{\rm q}(t)$ are seen, in the chaotic case, to relax faster towards 1.0 than they do in the integrable case. Third, the oscillation amplitudes of $S_{\rm q}(t)$ in the chaotic case are much smaller than that in the integrable case. Hence, the fast relaxation and small-amplitude oscillations of $S_{\rm q}(t)$ shown in Fig. 4 may be regarded as fingerprints of the underlying classical chaos. Finally, and most importantly, the entire time dependence, including oscillations in Figs. 3 and 4 of $S_{\rm q}(t)$ are beautifully captured by both the exact and the approximate $S_c(t)$. It should also be noted that the QCC time scale shown in Fig. 4 is appreciably longer than is the QCC break time $t_b\sim5.0$ for the same $\hbar$, obtained by quantitatively

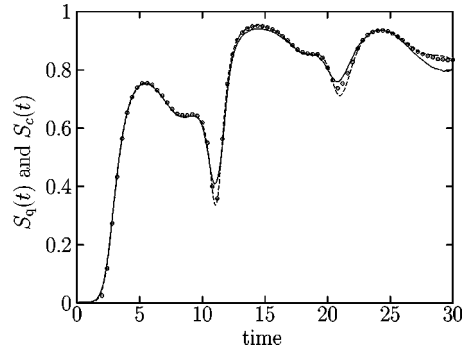

FIG. 3. A comparison between $S_{\rm q}(t)$ (dashed line) and the approximate $S_c(t)$ (solid line) calculated from Eq. (30) for the quartic oscillator model in the case of integrable dynamics ($\alpha=0.03,\beta=0.01$). The initial state is given by Eq. (26), with $\sigma_P=\sigma_Q=\sigma_p=\sigma_q=\sqrt{\hbar/2}$, $\hbar=0.005$, $Q_0=0.4$, $P_0=0.5$, $q_0=0.6$, and $H(Q_0,P_0,q_0,p_0)=0.24$. Full classical results based upon Eq. (27) are represented by discrete circular points. All variables are in dimensionless units.

comparing the structure of the classical and quantum distribution functions [23]. This can be understood by the fact that $S_c(t)$ [or $S_{\rm q}(t)$] describes the reduced distribution functions $\tilde{\rho}_c(Q,P,t)$ [or $\tilde{\rho}_W(Q,P,t)$], which is insensitive to the fine structure of $\rho_c(Q,P,q,p,t)$ [or $\rho_W(Q,P,q,p,t)$].

Calculations for many other initial states confirm that the QCC results shown in Figs. 3 and 4 are typical, indicating that (a) the QCC is essentially exact over large time scales and (b) the simple classical theory of intrinsic decoherence dynamics introduced above provides a useful approximation to the exact results.

Figure 5 shows one case, however, where the approximate $S_c(t)$ and exact classical or quantum results differ quantitatively. Here the system is still the quartic oscillator model with $\alpha=1.0$, $\beta=0.01$, but with an initial state of special type. In particular, both the initial average position Q_0 and the initial average momentum P_0 are set to zero. Initial states of this type are called channel states [17], and effectively give rise to very weak coupling between the two subsystems over a considerably large time scale. Indeed, since at short times $df/d\overline{Q}\approx\Delta f(\overline{Q})/\Delta Q\approx0$ for $\overline{Q}\approx Q_0=0$, one obtains from Eqs. (22) and (23) that $1/\tau_{c,2}^2=1/\tau_{2,\rm q}^2\approx0$. Therefore the early-time intrinsic decoherence rate should be small, as seen

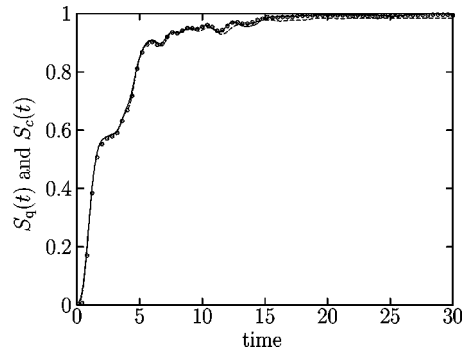

FIG. 4. Same as in Fig. 3 except for strongly chaotic dynamics ($\alpha=1.0,\beta=0.01$).

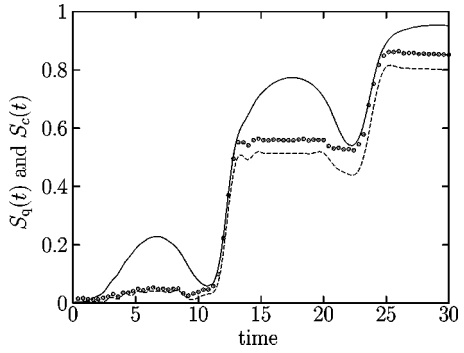

FIG. 5. Same as in Fig. 3 except for strongly chaotic dynamics ($\alpha=1.0,\beta=0.01$), and for a special initial Gaussian state, with $Q_0=P_0=0$, $q_0=0.6$, and $H(Q_0,P_0,q_0,p_0)=0.24$.

in Fig. 5, although the underlying classical dynamics is strongly chaotic. For this reason, one expects that the dynamical behavior of $S_c(t)$ and $S_q(t)$ should differ from previous cases. As shown in Fig. 5, in this case both $S_q(t)$ and $S_c(t)$ increase in a stepwise fashion, distinctly different from that in Figs. 3 and 4. Agreement between them remains excellent. However, the approximate $S_c(t)$ misses some of the important structure.

In Fig. 6, we show the QCC result for a simple variant of the quartic oscillator model, i.e., $V_{12}(Q,q)=0.5Q^2q^2+Q^4q^2$, a coupling potential that is neither linear nor quadratic. As seen in Fig. 6, even with such nonlinear coupling $S_c(t)$ and $S_q(t)$ are in excellent agreement over large time scales. This emphasizes the fact that the good QCC results observed in the quartic oscillator model are not due to the fact that the coupling potential therein is quadratic. Hence, we conclude that for initially localized states, our simple classical theory of intrinsic decoherence dynamics [see Eq. (30)] is generally useful in describing intrinsic decoherence dynamics in smooth Hamiltonian systems.

V. DISCUSSION AND SUMMARY

Quantum entanglement between individual subsystems has no classical analog. Nevertheless, as shown in this work, the quantum dynamics of quantum entanglement, as manifested in the quantum dynamics of intrinsic decoherence, does have a classical analog in classical Liouville dynamics

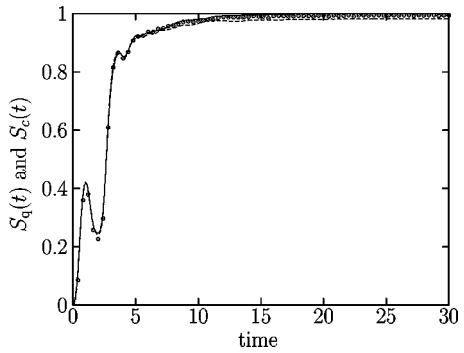

FIG. 6. Same as in Fig. 3 except for a modified quartic oscillator model in which $V_{12}(Q,q)=0.5Q^2q^2+Q^4q^2$.

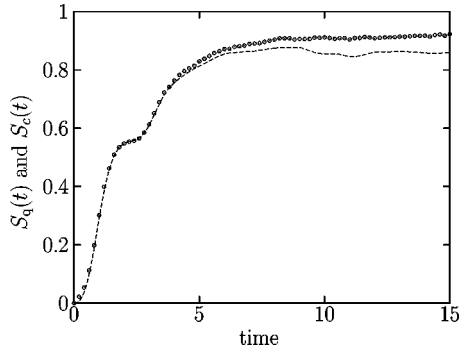

FIG. 7. A comparison between $S_q(t)$ (dashed line) and $S_c(t)$ (discrete circular points) for strongly chaotic dynamics of the quartic oscillator model ($\alpha=1.0,\beta=0.01$) and for $\hbar=0.05$. The initial state is given by Eq. (26), with $\sigma_P=\sigma_Q=\sigma_p=\sigma_q=\sqrt{\hbar/2}$, $Q_0=0.4$, $P_0=0.5$, $q_0=0.6$, and $H(Q_0,P_0,q_0,p_0)=0.24$. All variables are in dimensionless units.

describing classical correlations between classical subensembles. Hence, it is useful to isolate the conditions under which there is good QCC in intrinsic decoherence dynamics. This is done analytically, for early-time dynamics and for weak decoherence, by a second-order perturbative theory. Interestingly, as demonstrated by our computational studies in Secs. III and IV, the physical picture of the QCC afforded by the perturbative treatment can be still very useful even when the time scale under investigation is relatively long and the degree of intrinsic decoherence is significant. In particular, under the circumstances where there is good early-time QCC, classical Liouville dynamics can provide a simple means of understanding different aspects of intrinsic decoherence dynamics, for relatively large time scales and for both integrable and chaotic dynamics. Further, we have derived an approximate but very simple classical theory of linear entropy production of intrinsic decoherence dynamics associated with localized initial states, and shown that the rate of entropy production is closely related to the stability properties of classical trajectories.

Clearly, the linear entropy is just one of many possible representation-independent measures of intrinsic decoherence, and $S_q(t)\approx S_c(t)$ does not mean that the quantum dynamics is equivalent to the corresponding classical Liouville dynamics. For example, if the saturation value of the linear entropy in the long-time limit is of particular interest, then the measures $1/[1-S_c(t)]$ and $1/[1-S_q(t)]$ (which gives the number of orthogonal states that are incoherently populated) should be more useful in describing the QCC. Indeed, our results in Figs. 4 and 6 suggest that as time increases one has $1/[1-S_c(t)]\gg 1/[1-S_q(t)]$. This is consistent with our previous observation [8] that decoherence can dramatically improve QCC, but even strong decoherence does not necessarily suffice to ensure that quantum entropy production is the same as classical entropy production.

It should also be pointed out that the model quantum systems studied in this paper are still far from the semiclassical regime. This is indicated, in the chaotic case of the quartic oscillator model for example, by the fact that the QCC break time is relatively short compared to the time scale that we

examined. Correspondence will worsen quantitatively with increasing $\hbar$, although, as discussed above, $\hbar$ is far from the only factor influencing the quality of the QCC. However, we note that for localized initial states the qualitative features of the time dependence of classical and quantum linear entropies may remain similar to one another with much larger effective Planck constants. For example, Fig. 7 displays fairly good QCC between $S_q(t)$ and $S_c(t)$, in the chaotic case of the quartic oscillator model, with $\hbar = 0.05$ and with an initial symmetric Gaussian state.

A number of interesting extensions of this work are under consideration. First, it seems straightforward but necessary to consider cases in which the coupling potential depends upon both position and momentum. Second, we propose to further investigate the role of the dynamics of the subsystems in addition to that of the coupling potential (e.g., the dynamics in coupled Morse oscillator systems). Third, it is interesting to study the QCC in intrinsic decoherence dynamics in terms of the decay of off-diagonal density-matrix elements. Such studies are ongoing, with preliminary studies [24] indicating that comparing the time dependence of off-diagonal density-matrix elements to its direct classical analog [8] will provide deeper insights into the QCC in intrinsic decoherence dynamics.

To summarize, we have shown that classical dynamics can be very useful in describing intrinsic decoherence dynamics in smooth Hamiltonian systems. In particular, we have identified conditions under which excellent quantum-classical correspondence in the early-time dynamics of intrinsic decoherence is possible via a second-order perturbative treatment, have presented a simple classical theory of intrinsic decoherence dynamics emanating from localized initial states, and have provided supporting computational results. The hope is that by extending this study to high-dimensional Hamiltonian systems, we may use purely classical approaches to describe (at least qualitatively) the dynamics of quantum entanglement or intrinsic decoherence in polyatomic molecular systems.

ACKNOWLEDGMENTS

This work was supported by the U.S. Office of Naval Research and by the Natural Sciences and Engineering Research Council of Canada.

[1] W.H. Zurek, Rev. Mod. Phys. **75**, 715 (2003).
[2] V.S. Batista and P. Brumer, Phys. Rev. Lett. **89**, 143201 (2002).
[3] M.A. Nielsen and I.L. Chuang, *Quantum Computation and Quantum Information* (Cambridge University Press, Cambridge, 2000).
[4] M. Shapiro and P. Brumer, Adv. At., Mol., Opt. Phys. **42**, 287 (2000).
[5] S. A. Rice and M. Zhao, *Optical Control of Molecular Dynamics* (Wiley, New York, 2000).
[6] M. Shapiro and P. Brumer, *Principles of the Quantum Control of Molecular Processes* (Wiley, New York, 2003).
[7] J. Wilkie and P. Brumer, Phys. Rev. A **55**, 27 (1997); **55**, 43 (1997).
[8] J. Gong and P. Brumer, Phys. Rev. Lett. **90**, 050402 (2003); J. Gong and P. Brumer, e-print quant-ph/0212106.
[9] H. Wang, M. Thoss, K.L. Sorge, R.X. Giménez, and W.H. Miller, J. Chem. Phys. **114**, 2562 (2001); F. Grossmann, *ibid.* **103**, 3696 (1995); A.M.O. de Almeida, e-print quant-ph/0208094.
[10] P.C. Lichtner and J.J. Griffin, Phys. Rev. Lett. **37**, 1521 (1976); W.H. Zurek, S. Habib, and J.P. Paz, *ibid.* **70**, 1187 (1993); X-P. Jiang and P. Brumer, Chem. Phys. Lett. **208**, 179 (1993); A. Isar, A. Sandulescu, and W. Scheid, Phys. Rev. E **60**, 6371 (1999); G. Manfredi and M.R. Feix, *ibid.* **62**, 4665 (2000); J.N. Bandyopadhyay and A. Lakshminarayan, Phys. Rev. Lett. **89**, 060402 (2002).
[11] J.E. Moyal, Proc. Cambridge Philos. Soc. **45**, 99 (1949).
[12] J.I. Kim, M.C. Nemes, A.F.R. Toledo Piza, and H.E. Borges, Phys. Rev. Lett. **77**, 207 (1996).
[13] L.M. Duan and G.C. Guo, Phys. Rev. A **56**, 4466 (1997).
[14] D. Bacon, D.A. Lidar, and K.B. Whaley, Phys. Rev. A **60**, 1944 (1999).
[15] B. Eckhardt, G. Hose, and E. Pollak, Phys. Rev. A **39**, 3776 (1989).
[16] J. Gong and P. Brumer, Phys. Rev. E **60**, 1643 (1999).
[17] M.S. Santhanam, V.B. Sheorey, and A. Lakshminarayan, Phys. Rev. E **57**, 345 (1998).
[18] K. Furuya, M.C. Nemes, and G.Q. Pellegrino, Phys. Rev. Lett. **80**, 5524 (1998).
[19] P.A. Miller and S. Sarkar, Phys. Rev. E **60**, 1542 (1999).
[20] A. Lakshminarayan, Phys. Rev. E **64**, 036207 (2001).
[21] A. Tanaka, H. Fujisaki, and T. Miyadera, Phys. Rev. E **66**, 045201 (2002).
[22] M. Znidaric and T. Prosen, J. Phys. A **36**, 2463 (2003).
[23] J. Gong, Ph.D thesis, University of Toronto, 2001.
[24] H. Han, J. Gong, and P. Brumer (unpublished).